(Received 19 March 2025, Accepted 29 April 2025, Scheduled 8 May 2025)

Compact Wideband Reflective Phase Shifter with Wide Phase Shift Range and Simple Control

Teng Ma, Hongmei Liu*, Yuyang Jiang, and Zhongbao Wang

School of Information Science and Technology, Dalian Maritime University, Dalian 116026, Liaoning, China

ABSTRACT: In the paper, a planar wideband reflective phase shifter (RTPS) with wide phase shift range and simple control is proposed. It consists of a coupled-line based wideband 3-dB coupler and two multi-resonance reflective loads. By combining a series resonant circuit with a shunt resonant circuit to form multi-resonances, the phase shift range can be expanded with realizable capacitance values of the varactor diodes. The design equations are derived, and parametric analysis is provided. To verify the feasibility of the design methodology, an RTPS operating at the center frequency of 2 GHz is designed and fabricated. Measured results show that it exhibits a better than 10 dB input return loss bandwidth of 33.9% and a phase shift range of 320°. Besides, the size of the RTPS is only $0.41\lambda_g \times 0.13\lambda_g$, and can be controlled by simply one voltage.

1. INTRODUCTION

Reflective phase shifters (RTPSs) are widely used in various applications such as beamforming [1] and phased arrays [2]. Compact PSs with wide bandwidth and wide phase shift range have received increasing attention in recent years as the electronic steering of beams in phased arrays has increased, and the level of integration has improved [3].

RTPSs with a wide phase shift range have been widely studied in recent years. The main approaches are replacing series resonant loads with parallel resonant loads [4, 5], using π-network loads [6] or adding multi-resonant loads [7]. For example, the RTPS in [7] consists of a 90° Lange coupler and two multi-resonant loads to achieve a 360° phase shift range and 6.9% bandwidth. In [8], a triple-resonating load is proposed to achieve a full 360° phase shift range and suppress loss variations. In [9], the reported RTPS consists of a single layer double loaded coupled line coupler loaded with two varactor tuned circuits, which achieves a phase shift range of 392°. In recent years, there are some new methods that can also increase the phase shift range, such as the work in [10], where a two-branch switching network is cascaded to achieve a phase shift range of 360°. The RTPS proposed in [11] uses Magic-T to enhance the performance of the PS and achieves a phase shift range of 340°. However, although the above methods are effective for improving the phase shift range, because their operation bandwidth is narrow, they are not suitable for wideband communication system applications.

For widening the bandwidth, some scholars have used coupled line structures [12, 13]. The RTPS studied in [13] obtains a bandwidth of 20% by using coupled line, but the phase shift is only 146.93°. In [14], by connecting a lossless matching network with arbitrary output impedance in series with a varactor diode, the bandwidth of 25.3% is obtained. However, the phase shift is reduced to 118°. In [15], a novel design method for wideband tunable PSs is proposed, where the phase properties of coupled line and reflection load are both taken into consideration. The two designs realize the bandwidths of 33% and 55.6%. In [16], a capacitively loaded coupled line is proposed for constructing the RTPS, and a bandwidth of 30% is obtained. However, due to the goals of low phase error, the phase shift ranges are limited to 120°/135° [15] and 115° [16]. To obtain bandwidth and phase shift range enhancement, a vertically mounted planar structure is applied in the RTPS design [17]. It exhibits a bandwidth of 66.7% and a phase shift range of 127°. However, since this design is not planar, it does not meet the integration requirements of modern communication systems. Other researchers used a Magic-T structure [18] for designing the RTPS, where bandwidth and phase shift range reach 46% and 290°, respectively. However, this structure is complicated and costly in terms of processing materials and debugging. In the authors' previous work [19], a planar RTPS based on a trans-directional coupler is designed, which shows a bandwidth of 20% and a phase shift range of 425°. Although it has a wide phase shift range, the bandwidth is not enough for wideband applications.

To deal with this, the coupler in the RTPS should be replaced by a coupler with wider bandwidth, while its corresponding reflective loads should be modified in consideration of the phase performance of the wideband coupler. Thus, by applying a wideband coupler and connecting novel reflective loads, a compact wideband RTPS with wide phase shift range and simple control is proposed in this paper. Measurement results show that through voltage control arbitrary phase regulation among 320° is achieved within the bandwidth of 33.5%. Closed form equations are derived in Section 2, and the circuit parameters are analyzed in Section 3. For verification, a prototype operat-

* Corresponding author: Hongmei Liu (lhm323@dlmu.edu.cn).

ing at 2 GHz is fabricated and measured in Section 4. Finally, conclusions are given in Section 5.

2. THEORETICAL ANALYSIS

The schematic of the proposed tunable RTPS is given in Fig. 1. It consists of a coupled-line based wideband 3-dB coupler [20] and two reflective loads shunt on its through and coupled ends. It should be noted that for achieving a reduced size of the RTPS, the four open-circuited stubs in [20] are replaced by capacitor C_2 as shown in Fig. 1. Each reflective load is a multi-resonance circuit composed by two identical inductors (L_2) and three identical varactor diodes (D_1). Each inductor L_2 is connected in series with a varactor diode D_1 to form a series resonant circuit, and a third varactor diode D_1 is connected in parallel with the above two series resonant circuits to form a parallel resonant circuit. By combining the series resonant circuit with the shunt resonant circuit, the equivalent capacitance of the varactor diodes is increased, and the phase shift range is expanded.

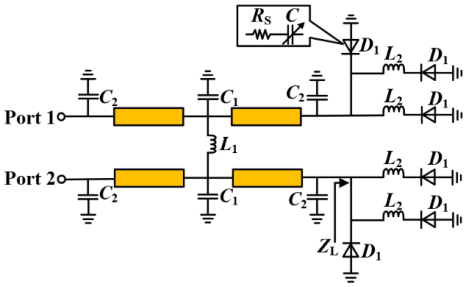

FIGURE 1. Schematic of the proposed tunable RTPS.

To facilitate the analysis, the varactor diode D_1 is equivalent to a parasitic resistor R_s series with an adjustable capacitor C, as shown in Fig. 1. Equation (1) gives the input impedance Z_L of the reflected load

$$Z_L = \frac{M_1 + \mathrm{j}M_2}{M_3/Z_0 + \mathrm{j}M_4/Z_0} \tag{1}$$

Then, the reflection coefficient can be obtained

$$\Gamma = \frac{Z_L - Z_0}{Z_L + Z_0} = |\Gamma| e^{\mathrm{j}\varphi} \tag{2a}$$

$$\varphi = \arctan \frac{\begin{array}{l}(M_1 + M_3)(M_2 - M_4) \\ -(M_1 - M_3)(M_2 + M_4)\end{array}}{\begin{array}{l}(M_1 - M_3)(M_1 + M_3) \\ +(M_2 - M_4)(M_2 + M_4)\end{array}} \tag{2b}$$

$$|\Gamma| = \frac{\sqrt{\begin{array}{l}[(M_1 - M_3)(M_1 + M_3) \\ +(M_2 - M_4)(M_2 + M_4)]^2 \\ +[(M_1 + M_3)(M_2 - M_4) \\ -(M_1 - M_3)(M_2 + M_4)]^2\end{array}}}{(M_1 + M_3)^2 + (M_2 + M_4)^2} \tag{2c}$$

where

$$M_1 = \omega^2 R_S^2 C^2 + \omega^2 L_2 C - 1 \tag{3a}$$

$$M_2 = \omega^3 L_2 R_S C^2 - 2\omega R_S C \tag{3b}$$

$$M_3 = 3Z_0 \omega^2 R_S C^2 \tag{3c}$$

$$M_4 = Z_0(\omega^3 L_2 C^2 - 3\omega C) \tag{3d}$$

According to (2), the maximum phase shift and insertion loss of the RTPS can be defined as $\Delta\varphi = |\varphi_{\max} - \varphi_{\min}|$ and $|S_{21}|^2$ (dB) $= -20\lg|\Gamma|$, respectively. Here, $\varphi_{\max}$ is the maximum phase shift, and $\varphi_{\min}$ is the minimum phase shift. According to the expressions of $\Delta\varphi$ and $|S_{21}|$, it can be found that they are mainly affected by the capacitance of varactor diode C and inductance L_2. Thus, curves of maximum phase shift and insertion loss versus the varactor diode C and inductance L_2 can be plotted, and as a result, suitable values can be chosen.

3. PARAMETRIC STUDIES

In this section, the impacts of the varactor capacitance C and inductance L_2 on the phase shift and insertion loss of the proposed RTPS are investigated. The center frequency is assigned as 2 GHz.

Figure 2 gives the phase shift of the RTPS when L_2 and C are within the ranges of 6 nH $\sim$ 16 nH and 0 pF $\sim$ 10 pF respectively. When C is varied from 0 pF to 4 pF, the phase shift range changes by about 450°. However, when C is varied from 5 pF to 10 pF, the phase shift range changes by about 30°. Therefore, the range of capacitance C is selected within 0 pF $\sim$ 4 pF. Also it is seen that the larger the value of inductor L_2 is taken, the steeper the phase shift curve is. When capacitance C is varied from 0 pF to 1 pF, the phase shift range changes by 165° with $L_2 = 6$ nH and 337° with $L_2 = 16$ nH. Thus, the value of L_2 is larger for better performance.

Figure 3 gives the insertion loss of the RTPS when L_2 and C change. It is seen that the maximum insertion loss decreases as the inductance L_2 increases. The range of insertion loss is

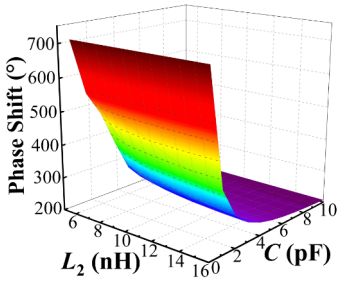

FIGURE 2. Phase shift range versus C and L_2.

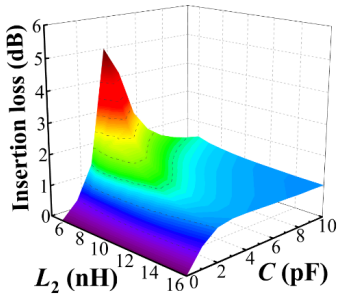

FIGURE 3. Insertion loss versus C and L_2.

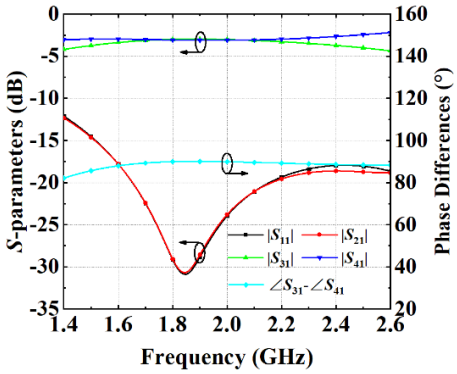

FIGURE 4. S-parameters of the couplers.

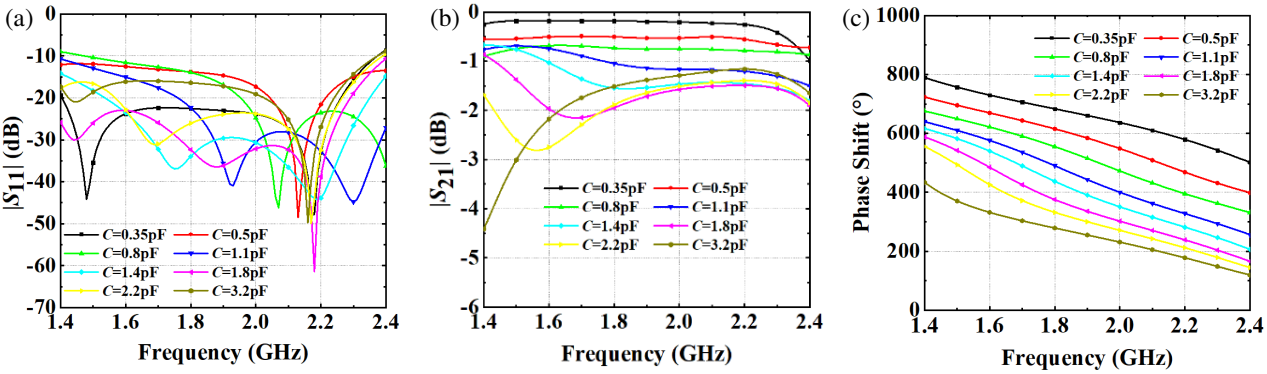

FIGURE 5. Theoretical results of the designed RTPS, (a) return loss, (b) insertion loss, (c) phase shift.

0 dB $\sim$ 5.14 dB when inductance L_2 is less than 10 nH, and the range of insertion loss is 0 dB $\sim$ 1.97 dB when inductance L_2 is greater than 10 nH. Thus, taking the phase shift range and insertion loss curves into consideration, the range of L_2 should be between 10 nH and 16 nH.

In summary, the design steps of the proposed RTPS are summarized as follows:

(1) Assign the design goals such as center frequency, phase shift range, and insertion loss.

(2) Plot the curves of phase shift and insertion loss versus different L_2 and C according to (2), and select suitable values of C and L_2.

(3) Modelling in ADS software from Keysight Technologies for simulation optimization and layout design.

(4) The parameter values are converted to the dimensions of the actual microstrip line using the calculation tool in ADS, modelled and simulated for optimization in HFSS software from ANSYS.

4. IMPLEMENTATION AND RESULTS

For validation, a prototype is designed at 2 GHz. Firstly, Fig. 4 gives the theory results of the coupler. In the range of 1.52 GHz $\sim$ 2.39 GHz (44.5%), the return loss and isolation are both larger than 15 dB, and the amplitude imbalance is less than 1 dB. Then, according to Figs. 2 and 3, the capacitance of the diode C is determined to be varied within 0.35 pF $\sim$ 3.2 pF, and the inductance L_2 is selected as 12 nH. By cascading the reflection load with the coupler, the proposed RTPS is constructed. Fig. 5 gives the theoretical simulation results using ADS. It is seen from Fig. 5(a) that the return loss is always greater than 10 dB in the frequency range of 1.57 GHz $\sim$ 2.36 GHz (40.2%), while according to Figs. 5(b) and (c), the insertion loss is less than 3 dB in the frequency range, and the phase shift range reaches 406°.

The prototype is modeled and implemented using an F4B substrate ($\varepsilon_r = 3.5$, $\tan\delta = 0.003$, $h = 1.5$ mm). The layout and photograph of the fabricated RTPS are given in Fig. 6. As shown in Fig. 6(b), the overall size of the RTPS is 37 mm $\times$ 12 mm, yielding $0.41\lambda_g \times 0.13\lambda_g$. Table 1 shows the final dimensions and component values. The SMV2020-079LF ($C_{\min} = 0.35$ pF, $C_{\max} = 3.2$ pF) from Skyworks is used as the varactor diode, where the parasitic resistance R_s is 2.5 Ω, and the bias voltage range is 0 V $\sim$ 20 V. The capacitors C_1 and C_2

TABLE 1. Physical dimensions of the RTPS (Unit: mm).

w_1	w_2	w_3	w_4	w_5	w_v	l_1
1.8	3.7	1	1.5	1.8	1.5	18
l_2	l_3	l_4	l_5	l_v	s_1	C_1
5	2	4	9	2.5	0.2	1.8 pF
C_2	L_1	L_2				
1 pF	2.7 nH	12 nH				

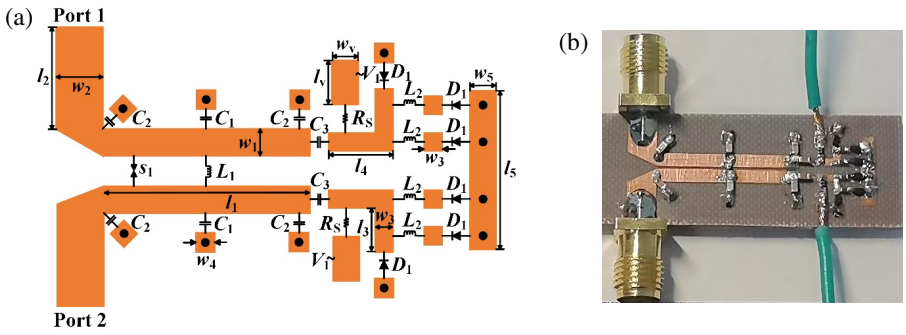

FIGURE 6. (a) Layout and (b) photograph of the RTPS.

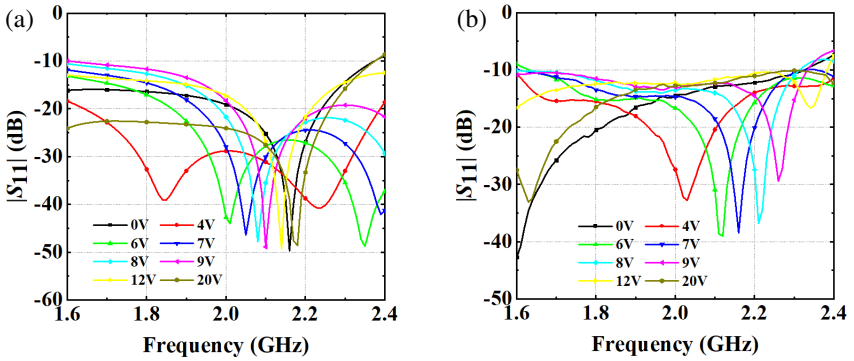

FIGURE 7. (a) Simulated and (b) measured $|S_{11}|$ of the proposed RTPS.

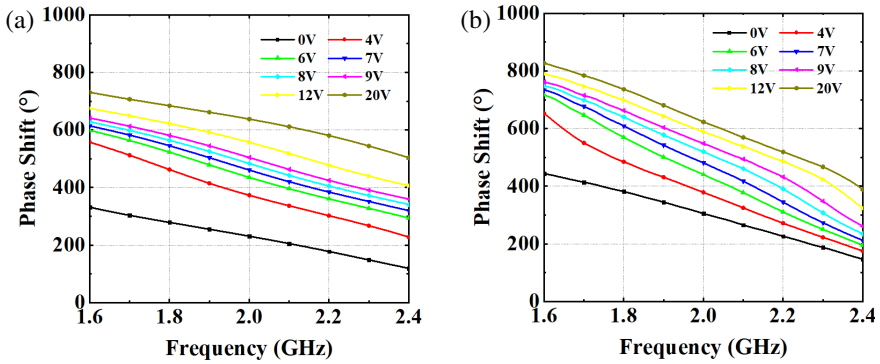

FIGURE 8. (a) Simulated and (b) measured phase shifts of the proposed RTPS.

are replaced by the commercially available Murata GRM1555 series, and the inductors L_1 and L_2 are replaced by the Murata LQW15 series. The values of the DC blocking capacitors C_3 and bias resistor R_{bias} are 2.2 nF and 10 kΩ respectively.

The prototype was measured using an Agilent N5230A. Figs. 7–9 show the simulated and measured results in the range of 1.6 GHz ∼ 2.4 GHz. From Fig. 7, it is seen that the simulated and measured 10 dB input return loss bandwidths are 1.61 GHz ∼ 2.3 GHz (35.3%) and 1.64 GHz ∼ 2.31 GHz (33.9%) when the reverse voltage is varied from 0 V to 20 V. From Fig. 8, it is found that the measured and simulated phase shift ranges are 320° and 400°, respectively. According to Fig. 9, the simulated and measured maximum insertion losses at the center frequency are 3.6 dB and 4.72 dB. It is noted that there is a certain deviation between the simulated and measured results. One reason is component error (typically 5%), especially when the actual equivalent capacitance value of the purchased varactor diode does not meet the specification, which will affect the phase shift magnitude. In addition, clutter and processing in the actual voltage source can affect the parasitic parameters of the varactor diode and capacitor inductors, increasing the insertion loss.

Table 2 shows the performances comparison between the proposed and reported RTPSs. The bandwidth of the RTPS mentioned in this paper is three times wider than that of [6] and four times wider than that of [10]. The phase shift range is almost tripled, and the bandwidth is wider than [13] and [16]. At the same time, the dimension of the proposed RTPS is smaller than those mentioned in [6, 10, 13]. Compared to the design with a 20% bandwidth [19], the bandwidth is increased by 69.5% for the current design. Although the work in [17] has wider bandwidth, the RTPS in this paper has almost three times

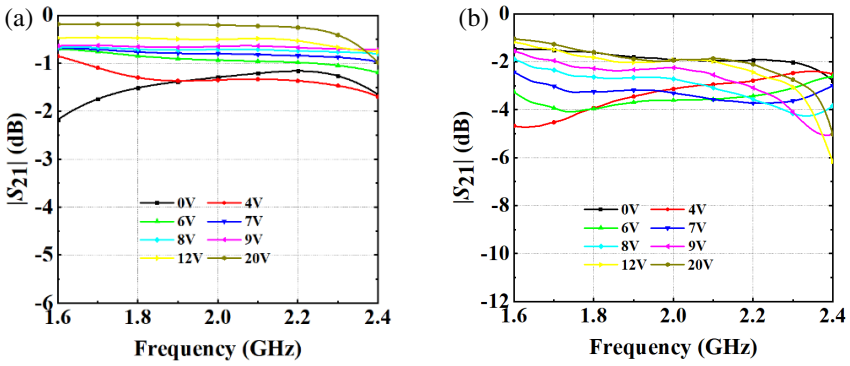

FIGURE 9. (a) Simulated and (b) measured insertion loss of the proposed RTPS.

TABLE 2. Performances comparison between the proposed and reported RTPSs.

Ref.	Freq. (GHz)	Phase shift range (°)	10-dB Bandwidths (%)	Size (λ_g^2)
[6]	2	385	11	0.11
[10]	2.45	360	8.1	0.21
[13]	2.5	146.9	20	0.11
[16]	2	115	30	0.016
[17]	1.5	127	66.7	0.10
[19]	2	425	20	0.05
This work	2	320	33.9	0.05

of the phase shift range. Moreover, the RTPS designed in this paper is a planar structure, which is simpler to process than the VIP structure in [17]. In addition, the proposed RTPS is controlled by only one voltage, which is more convenient to regulate. In conclusion, the RTPS proposed in this paper has the features of wide bandwidth, large phase shift range, small size, and simple control, which can be well applied to phased array systems and wireless communication systems.

5. CONCLUSION

In the paper, a compact planar wideband RTPS with wide phase shift range and simple control is proposed. A detailed theoretical analysis is given, and the parameters are investigated. Measurement results show that the RTPS achieves a 10 dB input return loss bandwidth of 33.9% with the phase shift range of 320°. Because the proposed RTPS has the advantages of wide bandwidth, wide phase range small size, and simple structure, it can be served as a candidate in modern communication devices, such as phased arrays and multibeam antennas.

ACKNOWLEDGEMENT

This work was supported in part by the National Natural Science Foundation of China under Grant 52471371, in part by the China Scholarship Council under Grant 202406570025, in part by the Young Elite Scientists Sponsorship Program by CAST under Grant 2022QNRC001, and in part by the Fundamental Research Funds for the Central Universities under Grant 3132024239.

REFERENCES

[1] Ren, H., P. Li, Y. Gu, and B. Arigong, "Phase shifter-relaxed and control-relaxed continuous steering multiple beamforming 4 × 4 Butler matrix phased array," *IEEE Transactions on Circuits and Systems I: Regular Papers*, Vol. 67, No. 12, 5031–5039, Dec. 2020.

[2] Omam, Z. R., W. M. Abdel-Wahab, A. Raeesi, A. Palizban, A. Pourziad, S. Nikmehr, S. Gigoyan, and S. Safavi-Naeini, "Ka-band passive phased-array antenna with substrate integrated waveguide tunable phase shifter," *IEEE Transactions on Antennas and Propagation*, Vol. 68, No. 8, 6039–6048, Aug. 2020.

[3] Arruela, R., T. Varum, and J. N. Matos, "Design of a compact Ka-band reflection-type vector modulator phase shifter," *IEEE Microwave and Wireless Technology Letters*, Vol. 34, No. 1, 53–56, Jan. 2024.

[4] Kirillov, V., D. Kozlov, and S. Bulja, "Series vs parallel reflection-type phase shifters," *IEEE Access*, Vol. 8, 189 276–189 286, 2020.

[5] Singh, A. and M. K. Mandal, "Electronically tunable reflection type phase shifters," *IEEE Transactions on Circuits and Systems II: Express Briefs*, Vol. 67, No. 3, 425–429, Mar. 2020.

[6] Burdin, F., Z. Iskandar, F. Podevin, and P. Ferrari, "Design of compact reflection-type phase shifters with high figure-of-merit," *IEEE Transactions on Microwave Theory and Techniques*, Vol. 63, No. 6, 1883–1893, Jun. 2015.

[7] Basaligheh, A., P. Saffari, S. R. Boroujeni, I. Filanovsky, and K. Moez, "A 28–30 GHz CMOS reflection-type phase shifter with full 360° phase shift range," *IEEE Transactions on Circuits and Systems II: Express Briefs*, Vol. 67, No. 11, 2452–2456, Nov. 2020.

[8] Gu, P. and D. Zhao, "Geometric analysis and systematic design of a reflective-type phase shifter with full 360° phase shift range and minimal loss variation," *IEEE Transactions on Microwave Theory and Techniques*, Vol. 67, No. 10, 4156–4166, Oct. 2019.

[9] Venter, J. J. P., T. Stander, and P. Ferrari, "X-band reflection-type phase shifters using coupled-line couplers on single-layer RF PCB," *IEEE Microwave and Wireless Components Letters*, Vol. 28, No. 9, 807–809, Sep. 2018.

[10] Guan, C.-E. and H. Kanaya, "360° phase shifter design using dual-branch switching network," *IEEE Microwave and Wireless Components Letters*, Vol. 28, No. 8, 675–677, Aug. 2018.

[11] Tamura, J. and H. Arai, "A broadband reflection-type phase shifter with low loss variation using magic-T and anti-phase reflection loads," in *2023 IEEE/MTT-S International Microwave Symposium — IMS 2023*, 1054–1057, San Diego, CA, USA, 2023.

[12] Abbosh, A. M., "Compact tunable reflection phase shifters using short section of coupled lines," *IEEE Transactions on Microwave Theory and Techniques*, Vol. 60, No. 8, 2465–2472, Aug. 2012.

[13] An, B., G. Chaudhary, and Y. Jeong, "Wideband tunable phase shifter with low in-band phase deviation using coupled line," *IEEE Microwave and Wireless Components Letters*, Vol. 28, No. 8, 678–680, Aug. 2018.

[14] Müller, D., A. Haag, A. Bhutani, A. Tessmann, A. Leuther, T. Zwick, and I. Kallfass, "Bandwidth optimization method for reflective-type phase shifters," *IEEE Transactions on Microwave Theory and Techniques*, Vol. 66, No. 4, 1754–1763, Apr. 2018.

[15] Lyu, Y.-P., L. Zhu, S.-T. Wang, and C.-H. Cheng, "A new synthesis method to design broadband continuously tunable phase shifters based on coupled line with low phase error," *IEEE Transactions on Microwave Theory and Techniques*, 1–10, 2024.

[16] Liu, F., J. Xu, J.-Y. Pu, J.-H. Su, and L. Zhu, "A hybrid architecture 360° phase shifter with continuously tunable phase shift and low in-band phase error," *IEEE Transactions on Microwave Theory and Techniques*, Vol. 72, No. 8, 4810–4821, Aug. 2024.

[17] Liu, W. J., S. Y. Zheng, Y. M. Pan, Y. X. Li, and Y. L. Long, "A wideband tunable reflection-type phase shifter with wide relative phase shift," *IEEE Transactions on Circuits and Systems II: Express Briefs*, Vol. 64, No. 12, 1442–1446, Dec. 2017.

[18] Tamura, J. and H. Arai, "A miniaturized magic-T using microstrip-to-coplanar strips transition and its application to a reflection-type phase shifter," *IEEE Transactions on Microwave Theory and Techniques*, Vol. 72, No. 3, 1810–1821, Mar. 2024.

[19] Liu, H., X. Wang, T. Zhang, S.-J. Fang, and Z. Wang, "Design of full-360° reflection-type phase shifter using trans-directional coupler with multi-resonance loads," *Progress In Electromagnetics Research Letters*, Vol. 101, 63–70, 2021.

[20] Liu, H., M. Guan, H. Zhang, S. Fang, and Z. Wang, "Compact wideband and harmonic suppressed quadrature coupler using susceptance loaded coupled lines," *Microwave and Optical Technology Letters*, Vol. 64, No. 3, 507–514, Dec. 2022.